

# DYNAMIC MODELING WITH CONDITIONAL QUANTILE TRAJECTORIES FOR LONGITUDINAL SNIPPET DATA, WITH APPLICATION TO COGNITIVE DECLINE OF ALZHEIMER'S PATIENTS<sup>†\*</sup>

Matthew Dawson<sup>1</sup> and Hans-Georg Müller<sup>2</sup>

<sup>1</sup> Graduate Group in Biostatistics, University of California, Davis

<sup>2</sup> Department of Statistics, University of California, Davis  
Davis, CA 95616 USA

June 2016

## ABSTRACT

Longitudinal data are often plagued with sparsity of time points where measurements are available and the functional data analysis perspective provides an effective and flexible approach to address this problem. The commonly studied case is where measurements are sparse but their times are randomly distributed over an interval. Here we focus on a different scenario where available data can be characterized as snippets, which are very short stretches of longitudinal measurements. For each subject the stretch of available data is much shorter than the time frame of interest. An added challenge is introduced if a time proxy that is basic for usual longitudinal modeling is not available. This situation arises in the case of Alzheimer's disease and comparable scenarios, where one is interested in time dynamics of declining performance, but the time of disease onset is unknown and the chronological age does not provide a meaningful time proxy for longitudinal modeling. Our main methodological contribution is to address this problem with a novel approach to obtain uniformly consistent estimates of conditional quantile trajectories for monotonic processes as solutions of a dynamic system. These trajectories are useful to describe processes that quantify deterioration over time, such as hippocampal volumes in Alzheimer's patients.

**KEY WORDS:** Functional data analysis, autonomous differential equations, uniform convergence, monotonic processes, nonparametric estimation, hippocampal volume.

---

<sup>†</sup> This research was supported by NSF grants DMS-1228369 and DMS-1407852.

\* The data used in this paper are from the Alzheimer's Disease Center at University of California Davis, supported by NIH and NIA grant P30 AG10129

## 1. INTRODUCTION

When adopting the functional approach to the analysis of longitudinal data, a common assumption is that the observations originate from a smooth underlying process. This assumption is justified, for example, when the observations correspond to biological mechanisms which are known to vary smoothly. For this reason, much attention has been given to modeling longitudinal data using a functional data analysis (FDA) perspective where a smoothness assumption is often welcomed. A common methodological challenge in such longitudinal studies, however, is that many studies lack complete and densely spaced observations over time. Some authors have explored this problem, for example Yao et al. (2005) focused on building a bridge between sparse longitudinal data and FDA; Kraus (2015) examined functional missingness in the case of otherwise dense data; Delaigle and Hall (2013) constructed a functional classifier in the presence of overlapping but partially censored curve fragments. So there are two existing approaches for sparsely measured functional data that differ substantially.

In this paper, we consider a third approach that substantially differs from the two previous ones. Some data generated in longitudinal studies exhibit an extreme form of sparseness and we refer to such data as snippet data. Such data can be characterized as very short longitudinal measurements relative to the domain of interest. Recovery of the underlying dynamics has not been systematically studied so far. Another layer of complexity in the analysis of snippet data is added if the time over which the measurements are taken is not meaningful on an absolute time scale since the origin of time is not known (such as disease onset) but can only be used to infer time differences on a short scale. This can happen, for instance, when measurements are taken with respect to age but the actual time axis of interest is time since disease onset, which may be unknown. Specifically, for snippet data, the functional completion method of Delaigle and Hall (2013) is not valid, and the covariance is not estimable which also precludes the methods of Yao et al. (2005)

and Kraus (2015). To demonstrate these issues we first examine a motivating dataset.

It is well established in the Alzheimer's disease (AD) literature that the hippocampus is affected for those suffering from Alzheimer's and dementia. The hippocampus is a region in the brain associated with memory and while it deteriorates in all people over time, it is known that the decline in volume is more rapid for AD patients, making hippocampal volume an important biomarker in Alzheimer's diagnosis (see for instance Mu and Gage (2011)). Naturally, our interest lies in modeling the hippocampal volume longitudinally. Here we take the response to be the log hippocampal volume which is the log of the sum of the hippocampal lobe volumes (left and right).

An unfortunate aspect of AD is that it can only be diagnosed post-mortem. As such, there is no way of knowing which patients have AD; we can only gain insight via cognitive tests. The subjects in this study have been classified in a clinical evaluation as having normal cognitive function, mild cognitive impairment, or dementia based on the SENAS (Spanish and English Neuropsychological Assessment Scales) cognitive test (see Mungas et al. (2004)). Information regarding the different clinical classifications may be found in Albert et al. (2011), McKhann et al. (2011), and Sperling et al. (2011).

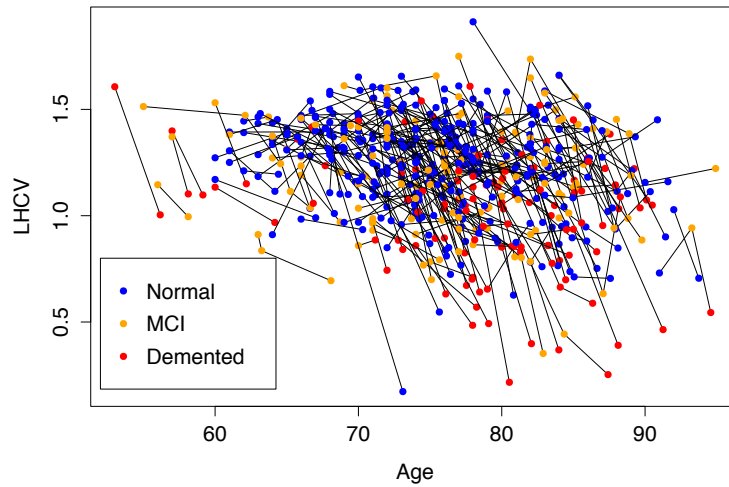


Figure 1: Log hippocampal volumes (LHCV) for all subjects with multiple measurements, colored by cognitive status: normal subjects are blue, those with MCI are orange, and demented subjects are shown in red.

Figure 1 displays some important features of the dataset. For example the measurements are clearly noisy, as several subjects have dramatic changes over short periods of time. More importantly, one has difficulty separating groups in terms of mean decline as the data form a cloud with no clear patterns. In particular, it is not entirely obvious whether there is an overall decrease over time. We claim that in fact, there is a clear difference between groups and that the rate of hippocampal atrophy is more dramatic than Figure 1 implies.

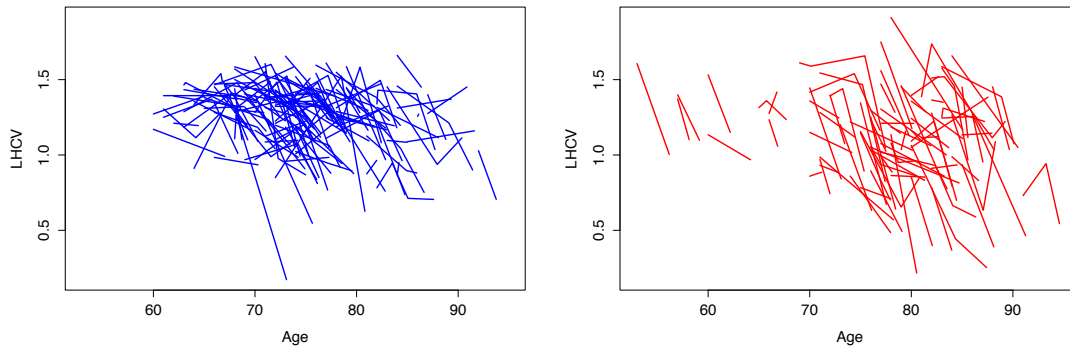


Figure 2: LHCV longitudinal measurements for normal and demented cognitive groups showing a notable difference between groups.

It should be noted that as Figure 1 suggests, there are several subjects with different cognitive classifications over time. For simplification, we define the demented subjects as those with at least one demented classification; the MCI as not having a demented rating, but having at least one MCI classification; and the normal group as having no MCI nor demented ratings. The difference between the normal and demented groups, for example, is pronounced in Figure 2. While the rates of decline are almost uniformly more severe for the demented group, there seems to be little difference in the mean trend over time with respect to age. Exploratory analysis shows that neither level nor local slope, calculated using a least squares fit on each subjects' measurements, change significantly over chronological age for the demented group.

This feature is not unique to AD studies. For instance one may be interested in the growth patterns of tumors. Here the time of interest would not be age, but rather the time since the inception of the tumor. In more complete data, one could register the curves based on some landmark features. With our limited data, however, this is not feasible. We conclude that age is an uninformative time scale and with little information available to register the data, we must seek new methodology to bypass modeling with time directly.

In the case of monotonic processes, Abramson and Müller (1994) found that one can still obtain trajectory information over time as long as information about local level and slope is known for each subject. Furthermore, the authors suggest that data in this form can be viewed as bivariate data, where we observe level and slope at some random, unobserved time. Formally, we can write this as observing  $X_i = f(T_i)$  and  $Z_i = f'(T_i) + \epsilon_i$ , for  $i = 1, \dots, n$ , with i.i.d. noise  $\epsilon_i$  satisfying  $E(\epsilon) = 0$  and  $E(\epsilon^2) = \sigma^2 < \infty$ , and where  $f$  is a fixed, strictly monotonic function. The idea is that for a monotonic function, there exists a function  $g$  that relates the slope to the level:  $f'(t) = g(f(t))$ , where  $g(x) = E(Z|X = x)$  and we can use the data to estimate this function using scatterplot smoothers. This approach is justified as with snippet data, we essentially observe local level and derivative information. For example, one can take the sample mean to obtain the level for each subject, and use a simple linear least squares fit to estimate the derivative.

A key assumption in Abramson and Müller (1994) is that we observe noisy measurements from a fixed function  $f$ . This implies that every subject must follow along the same population curve and is therefore not very realistic. We extend these methods by allowing observations to come from realizations of a stochastic process, and in contrast to Abramson and Müller (1994) we look to estimate functionals of the conditional distribution of slopes for a given level, rather than only the mean function.

The organization of this paper is as follows. In Section 2 we describe our dynamic model, while Section 3 covers estimation procedures. Our main theoretical results are discussed in Section 4. Simulations and an AD application are discussed in Sections 5 and 6, respectively.

## 2. DYNAMIC MODELING OF THE DISTRIBUTION OF DECLINE RATES

### 2.1. Basic Model

Assume that  $Y$  is a stochastic process that is  $k+1$ -times continuously differentiable for  $k \geq 1$ , defined on some domain  $\mathcal{T}_0$  and let  $\mathcal{J}$  be the range of  $Y$  restricted to  $\mathcal{T}_0$ . Measurements

are generated by observing  $Y(T_i)$  and  $Y'(T_i)$  at some random and unobserved time  $T_i$ . Denote these observations as  $X_i = Y(T_i)$  and  $Z_i = Y'(T_i)$  for  $i = 1, \dots, n$ . Further assume that  $T_i \sim f_T$  for some density  $f_T$  on  $\mathcal{T}_0$ , and that  $(X_i, Z_i, T_i)$  have a joint distribution and are independent of  $(X_j, Z_j, T_j)$  for  $i \neq j$ . A core feature of our model is that the conditional distribution of the slope given the level does not depend on  $T$ , which means that the distribution of the rate of decline depends only on the current level but not on the random time where the observation of level and slope takes place. That is,

$$F(z|x) = P(Y'(T) \leq z \mid Y(T) = x) = P(Z \leq z \mid X = x), \quad (1)$$

so that  $F(z|x)$  does not depend on anything else beyond  $z$  and  $x$ . This implies that the process is completely determined by the relationship between level and slope.

Rather than only aiming at the conditional mean, our goal is to target the distribution of slopes at a given level which then will provide insights into the dynamics of the process. Ultimately we target the conditional quantile trajectories of the process  $Y(t)$ , which describe the probabilistic time dynamics of the process  $Y$  given a starting point and provide a more comprehensive reflection of the underlying dynamics than the conditional expected trajectories alone. The assumption that the measurements are taken from realizations of a general stochastic process leads to increased flexibility in modeling and accounts for subject-specific variation.

Further examining the nature of (1), simple calculations show that monotonic functions with random components are included under the assumptions. These could for example be exponential or logarithmic curves with subject-specific random time shifts, time dilations, intercepts, and/or amplitudes. For a specific example, consider the model  $Y(t) = af(bt + c) + d$  where  $f(\cdot)$  is a fixed monotone function, and  $(a, b, c, d)$  is a random vector with some joint distribution. Examining the conditional probabilistic behavior of this process

at a randomly and independently selected time  $T$ , find

$$\begin{aligned} F(z|x) &= P(Y'(T) \leq z \mid Y(T) = x) \\ &= P(abf'(bT + c) \leq z \mid Y(T) = x) \\ &= P\left(abf'\left(f^{-1}\left(\frac{1}{a}Y(T) - \frac{d}{a}\right)\right) \leq z \mid Y(T) = x\right), \end{aligned}$$

so that  $F(z|x)$  is seen to depend only on  $x$  and  $z$ , whence the model assumptions are satisfied.

Note that in this example,  $F(z|x)$  depends on the random quantities  $(a, b, c, d)$ . However, the key observation is that the distribution of slopes at some random time  $T$  only depend on the level at that same time  $T$ . Therefore we can obtain inference for conditional probabilities involving  $Y'(T)$  without explicitly observing  $T$ . This is crucial because it implies that the time dependent process  $Y$  can be modeled without actually observing the unknown time.

## 2.2. Evolution of Conditional Distributions and Quantiles

Acquiring an estimate of (1) will provide insight into the instantaneous probabilistic dynamics of a process. From an applications standpoint, this conditional distribution tells us where subjects generally are headed in the immediate future, based on their starting level, not only in the mean but also including the distribution of their slopes of decline. One can readily compute other functionals from this conditional distribution, for example quantiles are naturally of interest.

In data applications it is additionally of interest to infer how the process behaves over a longer period of time, continuing after time  $T$ . The conditional mean function  $E(Y(T+t) \mid Y(T) = x)$ , for  $t \in \mathcal{T} = (0, \tau]$  for some  $\tau > 0$  has previously been studied by Abramson and Müller (1994), who aimed at estimating the overall mean curve assuming an initial value, rather than conditioning on any given starting point. To assess long

term behavior of the decline process after a random starting time  $T$ , we introduce the notion of an  $\alpha$ -quantile trajectory, for a given  $0 < \alpha < 1$ . To this end, we first define the *instantaneous  $\alpha$ -quantile* at a given level  $x$  as  $\xi_\alpha(x)$ , which is

$$\xi_\alpha(x) = F^{-1}(\alpha|x), \text{ where } F(z|x) = P(Y'(T) \leq z \mid Y(T) = x). \quad (2)$$

The function  $\xi_\alpha$  describes the  $\alpha$ -quantile of slope for a given level, providing information about the instantaneous rate of decline. A simple, yet useful way to utilize  $\xi_\alpha(x)$  is to define a class of trajectories such that at all times, they are following the  $\alpha$ -quantile of slope. In a sense, these are the curves that are always changing at the same rate relative to the conditional probability distribution. We define such a trajectory  $z_{\alpha,x}$  as the solution to an autonomous differential equation:

$$\frac{dz_{\alpha,x}(T+t)}{dt} = \xi_\alpha(z_{\alpha,x}(T+t)) \quad (3)$$

with initial condition  $z_{\alpha,x}(T+0) = x$ . We then refer to the function  $z_{\alpha,x}(\cdot + t)$  as the  *$\alpha$ -quantile trajectory* and note that it depends only on  $t$  and  $x, \alpha$  but does not depend on the random time  $T$ .

Note that  $\xi_\alpha$  is the gradient function relating the slope to the level. Defining a quantile trajectories in this way sidesteps  $T$ , which is unknown. This approach can be contrasted with Abramson and Müller's strategy for estimating the conditional mean function  $\mu_x(T+t)$ , which is the function satisfying

$$\frac{d\mu_x(T+t)}{dt} = E(Y'(T+t) \mid Y(T) = \mu_x(T+t)), \quad (4)$$

with initial condition  $\mu_x(T+0) = x$ . It is straightforward to can estimate the  $\alpha$ -quantile trajectories iteratively, using simple numerical integration techniques, such as Euler's

method, to solve the defining autonomous differential equation (3).

An alternative way of characterizing the distribution of the process would be to target cross-sectional quantiles. That is, define  $G_t$  as the function

$$G_t(y|x) = P(Y(T+t) \leq y \mid Y(T) = x), \quad (5)$$

the distribution of  $Y(T+t)$  for a given starting value. Taking the  $\alpha$ -quantile for all  $t \in \mathcal{T}$  gives the *cross-sectional  $\alpha$ -quantile trajectory*

$$q_{\alpha,x}(T+t) = G_t^{-1}(\alpha|x). \quad (6)$$

The cross-sectional quantile  $q_{\alpha,x}$  thus explicitly depends on  $Y(T+t)$ , which is not observed. In general  $z_{\alpha,x}$  and  $q_{\alpha,x}$  will not be the same, due to basic differences in their definitions. However, according to Proposition 1 below, in many cases  $z_{\alpha,x}$  and  $q_{\alpha,x}$  will coincide. For this we will require some smoothness and uniqueness assumptions, where  $C^{k+1}$  is the space of  $k+1$ -times continuously differentiable functions for  $k \geq 1$ ,

(A1) The cross-sectional quantile trajectories  $q_{\alpha,x}$  satisfy  $q_{\alpha,x} \in C^{k+1}(\mathcal{T})$  and are monotone in  $t$ .

(A2) The cross-sectional quantiles are unique:  $G_t(y) = P(Y(T+t) \leq y \mid Y(T) = x)$  is strictly monotone in  $y$  for all  $t \in \mathcal{T}$ .

Assumption (A1) is necessary to ensure that the trajectory  $q_{\alpha,x}$  can be written as the solution to an autonomous differential equation, and implies that there exists a function  $h \in C^k(\mathcal{J})$ , where  $\mathcal{J}$  is the range of  $Y$  restricted to  $\mathcal{T}$ , so that  $q_{\alpha,x}$  is the solution to an autonomous differential equation

$$\frac{dq_{\alpha,x}(T+t)}{dt} = h(q_{\alpha,x}(T+t)).$$

The second assumption (A2) guarantees uniqueness of the cross-sectional quantiles so that  $q_{\alpha,x}$  is defined uniquely.

**Proposition 1.** *If the process  $Y$  satisfies (A1) and (A2), then  $\alpha$ -quantile cross-sectional trajectories and  $\alpha$ -quantile trajectories coincide, i.e.,  $q_{\alpha,x}(T+t) = z_{\alpha,x}(T+t)$  for all  $t \in \mathcal{T}$ .*

The implication is that under these smoothness and autonomous assumptions we may target  $z_{\alpha,x}$  and interpret it as a cross-sectional quantile. This allows us to investigate the conditional median, best and/or worst case scenarios, and all intermediate quantiles, as we will demonstrate in the simulations in section 5 and in the data examples in section 6.

### 3. ESTIMATION

#### 3.1. Estimation of Conditional Distributions and Quantiles

The task of estimating  $z_{\alpha,x}$  can be decomposed into three steps. First, we estimate the conditional distribution  $F(z|x)$ . Next we use this estimate to obtain an estimate of the instantaneous conditional quantile function  $\xi_\alpha$ , according to (2). Finally, this estimate of  $\xi_\alpha$  is employed as gradient function in an autonomous differential equation as per (3), and then this equation is solved numerically. The details are as follows.

The data in our application is of the form  $(X_i, Z_i)$  for  $i = 1, \dots, n$ . For a subject with  $n_i$  measurements  $Y_{ij}$  at ages  $A_{ij}$ ,  $j = 1, \dots, n_i$ , one may use the empirical estimators  $X_i = \frac{1}{n_i} \sum Y_{ij}$  and  $Z_i = \hat{\beta}_{1i}$ , where  $(\hat{\beta}_{0i}, \hat{\beta}_{1i}) = \operatorname{argmin}_{(\beta_{0i}, \beta_{1i})} \sum_{j=1}^{n_i} (Y_{ij} - \beta_{0i} - \beta_{1i}A_{ij})^2$ . We assume that observations between individuals are assumed to be independent, and in this setup, estimation of conditional distribution functions has been widely studied in the literature (see Hall et al. (1999), Li and Racine (2008), Roussas (1969), Samanta (1989), Ferraty et al. (2006), Horrigue and Saïd (2011), for example). Here we outline several methods by which one can estimate the conditional distributions  $F(z|x)$  defined in (1).

**Binomial regression.** One can write the conditional distribution function as  $F(z|x) = E(1(Z \leq z) \mid X = x)$ . Assuming linearity and a link function  $g$  we can model the

conditional distribution parametrically as

$$F(z|x) = E(1(Z \leq z) \mid X = x) = g^{-1}(\beta_0 + \beta_1 x + \beta_2 z). \quad (7)$$

Flexibility can be increased by making use of a generalized additive model

$$F(z|x) = E(1(Z \leq z) \mid X = x) = g^{-1}(\alpha_0 + f_1(x) + f_2(z)), \quad (8)$$

where  $f_1$  and  $f_2$  are assumed to be smooth with  $\int f_1 = \int f_2 = 0$ . These parametric methods are simple but require strong assumptions. For instance, the shape of the c.d.f. is determined by the unknown link function  $g$ . However, additional covariates can be included in a straightforward way, making this approach appealing for some applications.

**Empirical c.d.f. based on binning.** A basic approach for nonparametric estimation of a conditional distribution involving two continuous variables is to take a small window around the conditioning variable, selecting the data where the conditioning variable falls into the window, and computing the empirical c.d.f. based on these data. I.e., when estimating  $P(Z \leq z \mid X = x)$ , one can simply take a window  $\{x \pm h\}$  and calculate the empirical c.d.f. over  $Z$  for all subjects satisfying  $X \in \{x \pm h\}$ , or

$$\tilde{F}_B(z|x) = \frac{1}{n} \sum_{i=1}^n 1(Z_i \leq z) 1(X_i \in \{x \pm h\}). \quad (9)$$

This can be extended to include additional covariates but this may incur a curse of dimensionality depending on the number of covariates.

**Kernel smoothing.** A natural extension of binning is kernel smoothing, analagous to extending a histogram to a smooth density function estimate. This leads to estimators

$$\tilde{F}_K(z|x) = \frac{\sum_{i=1}^n 1(Z_i \leq z) K_h(x - X_i)}{\sum_{i=1}^n K_h(x - X_i)}, \quad (10)$$

where  $K_h(u) = h^{-1}K(u/h)$  and  $K$  is a kernel function, generally chosen as a smooth and symmetric probability density function. This estimator is well understood and is a simple extension of the binning method (9). Several variants of this estimator have been considered (see, for example, Hall et al. (1999) and Li and Racine (2008)).

**Joint kernel smoothing.** Finally, one might prefer an estimator that is differentiable in  $x$  as well as  $z$ . A smoothed version of (10) is obtained by replacing the indicator function with a smooth distribution function  $H$ :

$$\hat{F}_{JK}(z|x) = \frac{\sum_{i=1}^n H_{h_H}(z - Z_i)K_{h_K}(x - X_i)}{\sum_{i=1}^n K_{h_K}(x - X_i)}, \quad (11)$$

Here  $K_h$  is as before with bandwidth  $h_K$  and  $H_{h_H}(u) = H(u/h_H)$  with possibly different bandwidth  $h_H$ . For  $K$  one commonly uses a probability density function and  $H$  is its corresponding cumulative distribution function:  $H(u) = \int_{-\infty}^u K(t)dt$ . This type of estimator was studied in Roussas (1969) and Samanta (1989) and has since been extended to include functional predictors in Ferraty et al. (2006) and Horrigue and Saïd (2011). As we will require differentiability of our estimate of  $F(z|x)$ , we will use estimator (11) in our theoretical results and implementations.

Given an estimator  $\tilde{F}(z|x)$  of  $F(z|x)$  one can easily construct an estimate of  $\xi_\alpha$ ,

$$\tilde{\xi}_\alpha(x) = \inf\{z : \tilde{F}(z|x) \geq \alpha\}, \quad (12)$$

which we will denote by  $\hat{\xi}_\alpha(x)$  if it is based on  $\tilde{F}(z|x) = \hat{F}_{JK}(z|x)$  in (11). Our method for estimating  $z_{\alpha,x}(T+t)$  involves first using  $\tilde{\xi}_\alpha(x)$  in (12) as a plug-in estimate for  $\xi_\alpha(x)$  in (3), and then solving the resulting differential equation using numerical methods.

### 3.2. Numerical Integration of the Differential Equation

The final estimation step is using an estimate  $\xi_\alpha$  to produce an estimate of  $z_{\alpha,x}$ . To

estimate the solution of (3) we may use one of several iterative procedures such as Euler's method or the Runge-Kutta method, along with a uniformly consistent quantile estimate. We first discuss a numerical approximation to the solution  $z_{\alpha,x}(t+T)$ . Then we examine how this quantity can be estimated from the data. For the sake of simplifying notation, in all of the following we assume that  $T = 0$ , without loss of generality as  $z_{\alpha,x}$  does not depend on  $T$ . Then our target becomes  $z_{\alpha,x}(s)$  for  $s \in \mathcal{T} = (0, \tau]$  where now

$$\frac{dz_{\alpha,x}(s)}{ds} = \xi_{\alpha}(z_{\alpha,x}(s)) \quad (13)$$

with initial condition  $z_{\alpha,x}(0) = x$  to guarantee the quantile curve starts at the stipulated level  $x$ , and again with  $\xi_{\alpha}(x)$  as the  $\alpha$ -quantile of the distribution of  $Y'(T)$  given  $Y(T) = x$ .

An approximating solution to  $z_{\alpha,x}(\cdot)$  is given by  $\{s_i, \psi(s_i)\}$ ,  $i = 0, \dots, m$  for some  $m \in \mathbb{N}$  where these quantities are found iteratively using the rule

$$\psi(s_0) = x, \quad s_{i+1} = s_i + \delta, \quad \psi(s_{i+1}) = \psi(s_i) + \delta\Phi(\psi(s_i), \delta, \xi_{\alpha}), \quad (14)$$

where  $\delta$  is a small time increment. In the case of Euler's method, we have  $\Phi(\psi(s_i), \delta, \xi_{\alpha}) = \xi_{\alpha}(\psi(s_i))$ , while the Runge-Kutta approximation uses

$$\Phi(\psi(s_i), \delta, \xi_{\alpha}) = \frac{1}{6}(k_1 + 2k_2 + 2k_3 + k_4),$$

where  $k_1 = \xi_{\alpha}(\psi(s_i))$ ,  $k_2 = \xi_{\alpha}(\psi(s_i) + \delta k_1/2)$ ,  $k_3 = \xi_{\alpha}(\psi(s_i) + \delta k_2/2)$ ,  $k_4 = \xi_{\alpha}(\psi(s_i) + \delta k_3/2)$

To understand how the numerical solution  $\{s_i, \psi(s_i)\}$  converges, we consider for a pair  $(s^*, z_{\alpha,x}(s^*))$

$$\Delta(s^*, z_{\alpha,x}(s^*), \delta, \xi_{\alpha}) = \begin{cases} [z_{\alpha,x}(s^* - \delta) - z_{\alpha,x}(s^*)]/\delta & \text{if } \delta \neq 0 \\ \xi_{\alpha}(z_{\alpha,x}(s^*)) & \text{if } \delta = 0. \end{cases}$$

The local discretization error at a point  $(s^*, z_{\alpha,x}(s^*))$  is given by

$$LDE(s^*, z_{\alpha,x}(s^*), \delta) = \Delta(s^*, z_{\alpha,x}(s^*), \delta, \xi_\alpha) - \Phi(z_{\alpha,x}(s^*), \delta, \xi_\alpha). \quad (15)$$

Now let  $-\infty < a_1 < a_2 < \infty$ . The integration procedure defined by  $\Phi$  is of order  $q$ , for  $q \geq 1$  and  $q$  is an integer, on  $[a_1, a_2]$  if  $LDE(s, z_{\alpha,x}, \delta) = O(\delta^q)$  for all  $s \in [a_1, a_2]$ ,  $z_{\alpha,x} \in \mathbb{R}$  and for all  $g \in C_b^q(\text{range } z_{\alpha,x}|[a_1, a_2])$ , where  $C_b^q[c_1, c_2]$  denotes the real functions which are  $q$  times continuously differentiable and bounded  $q$ -th derivative on  $[c_1, c_2]$ , for  $-\infty \leq c_1 < c_2 \leq \infty$ . It is well known that Euler's method achieves order  $q = 1$ , while the Runge-Kutta approximation achieves order  $q = 4$  (Gragg (1965)).

Of course, the function  $\xi_\alpha(x)$  is unknown and must be estimated from the data. We plug in an estimate  $\tilde{\xi}_\alpha(x)$  into the right hand side of equation (3) and then carry out the numerical integration as described above. This leads to the estimating differential equation

$$\frac{d\tilde{z}_{\alpha,x}(s)}{ds} = \tilde{\xi}_\alpha(\tilde{z}_{\alpha,x}(s)), \quad (16)$$

for  $s \in \mathcal{T} = (0, \tau]$ , with initial condition  $\tilde{z}_{\alpha,x}(0) = x$ . Using the numerical integration outlined above in (14) for this differential equation gives the numerical solution  $\{s_i, \tilde{\psi}(s_i)\}$ . We establish that under regularity conditions, we obtain uniform consistency for  $\tilde{\psi}$  as an estimator of  $z_{\alpha,x}$  with the corresponding rate depending on the convergence rate of the integration procedure as well as the uniform convergence rate of the estimator  $\tilde{\xi}_\alpha(x)$ .

#### 4. THEORETICAL RESULTS

Our main result is Theorem 2 on uniform consistency of an arbitrary estimate  $\tilde{\psi}$  of  $z_{\alpha,x}$ , obtained through numerical integration. Theorem 1 provides consistency for the estimator  $\hat{F}_{JK}(z|x)$  and the associated estimator  $\hat{\xi}_\alpha$ . In particular, we show that  $\hat{F}_{JK}(z|x)$  satisfies the assumptions of Theorem 2 and therefore leads to a uniformly consistent estimator of  $z_{\alpha,x}$ . We require the following conditions:

(B1)  $\mathcal{J} = \text{range}(Y)|\mathcal{T}_0 = [c_1, c_2]$  and  $\mathcal{Z} = \text{range}(Y')|\mathcal{T}_0 = [d_1, d_2]$ , where  $\mathcal{T}_0$  is the time interval over which measurements are taken.

(B2)  $f_X(x)$ , the marginal density of  $X$ , and  $f_{X,Z}(x, z)$ , the joint density of  $(X, Z)$ , satisfy

$$0 < m_1 \leq \inf_{x \in \mathcal{J}} f_X(x) < \sup_{x \in \mathcal{J}} f_X(x) \leq M_1 < \infty$$

and

$$0 < m_2 \leq \inf_{x \in \mathcal{J}, z \in \mathcal{Z}} f_{X,Z}(x, z) < \sup_{x \in \mathcal{J}, z \in \mathcal{Z}} f_{X,Z}(x, z) \leq M_2 < \infty$$

for some constants  $m_1, m_2, M_1, M_2$ .

(B3) With  $F^{(i,j)}(x, z) = \frac{\partial^{i+j} F(x, z)}{\partial x^i \partial z^j}$ , where  $F(x, z)$  is the two-dimensional c.d.f. of  $(X, Z)$ , assume that  $F^{(i+p, j+p)}(x, z)$  exists and is bounded for  $(i, j) = (1, 0), (1, 1), (2, 0)$ . Also assume that  $f_X(x)$  is  $p + 1$  continuously differentiable.

(B4) The conditional quantiles are unique, i.e.  $F(z|x)$  is a strictly monotone function of  $z$  in a neighborhood of  $\xi_\alpha(x)$ .

(B5)  $H'(u) = K(u)$  and  $K$  is a symmetric, compactly supported kernel which is  $p$ -times continuously differentiable, of bounded variation, and satisfies  $\int uK(u)du = 0$  and  $\int u^2K(u)du < \infty$ .

(B6) The bandwidth  $h_K = h_H = h_n$  satisfies (i)  $\frac{\log n}{nh_n^2} \rightarrow 0$  as  $n \rightarrow \infty$ , (ii)  $h_n = o((\frac{\log n}{n})^{1/4})$ , and (iii) The series  $\sum_{n=1}^{\infty} \exp\{-\kappa nh_n^4\}$  is convergent for all  $\kappa > 0$ .

Assumptions (B1) - (B3) are standard assumptions regarding the smoothness and boundedness of the distributions when applying smoothing (see Ferraty et al. (2006), Hansen (2008), and Samanta (1989), for example). Assumption (B4) guarantees that the target quantiles are unique by stipulating that the conditional c.d.f. must not be flat near the quantile we are estimating. Finally, assumptions (B5) and (B6) are typical assumptions on the kernel and bandwidth for kernel estimators.

**Theorem 1.** *Under conditions (B1) - (B6), we have that the estimator  $\hat{\xi}_\alpha$ , defined at (12) and obtained by inverting  $\hat{F}_{JK}(z|x)$  in (11) satisfies*

$$\sup_{x \in \mathcal{J}} |\hat{\xi}_\alpha(x) - \xi_\alpha(x)| = O_p \left( h_n + \sqrt{\frac{\log n}{nh_n}} \right) \quad (17)$$

and

$$\sup_{x \in \mathcal{J}} |\hat{\xi}'_\alpha(x) - \xi'_\alpha(x)| = o_p(1). \quad (18)$$

For the proof of Theorem 1, one shows first that the estimator  $\hat{F}_{JK}(z|x)$  is well-behaved, whence the estimated driving function  $\hat{\xi}_\alpha$  of the autonomous differential equation in (16) and its derivative are seen to be consistent. For the following main result, some additional conditions are needed:

(C1) Assume that one has a continuously differentiable function  $\tilde{\xi}_\alpha$  satisfying

$$\sup_{x \in \mathcal{J}} |\tilde{\xi}_\alpha(x) - \xi_\alpha(x)| = O_p(\beta_n), \quad \sup_{x \in \mathcal{J}} |\tilde{\xi}'_\alpha(x) - \xi'_\alpha(x)| = O_p(1)$$

for a sequence  $\beta_n$  with  $\beta_n \rightarrow 0$ ,  $n\beta_n \rightarrow \infty$  as  $n \rightarrow \infty$ .

(C2) The function  $\Phi(y, \delta, \tilde{\xi}_\alpha)$  defining the numerical integration method (14) is continuous in its first two arguments on  $G = \{(y, \delta, \tilde{\xi}_\alpha) : |z_{\alpha,x}(s) - y| \leq \gamma, 0 \leq s \leq \tau, \delta \leq \delta_0\}$  for some given  $\gamma > 0$ ,  $\delta_0 > 0$  and satisfies  $|\Phi(y_1, \delta, \tilde{\xi}_\alpha) - \Phi(y_2, \delta, \tilde{\xi}_\alpha)| \leq L|\tilde{\xi}_\alpha(y_1) - \tilde{\xi}_\alpha(y_2)|$  for some  $L > 0$  and for all  $y_1, y_2, \delta \in G$ .

(C3) The integration method is of order  $q$ , i.e., the local discretization error satisfies

$$|LDE(s, y, \delta)| = |\Delta(s, y, \delta, \tilde{\xi}_\alpha) - \Phi(y, \delta, \tilde{\xi}_\alpha)| = O(\delta^q)$$

for  $s \in \mathcal{T}$ ,  $\delta \leq \delta_0$ ,  $y = z_{\alpha,x}(s)$ .

Assumption (C1) is quite natural, as we require the consistency of the gradient function estimate which drives our estimation and the condition on the derivative is needed to control the remainder in the local estimation error. Assumptions (C2) - (C3) deal with the smoothness and convergence of the numerical integration procedure. We note that both the Euler and Runge-Kutta methods satisfy these requirements.

**Theorem 2.** *For an estimator  $\tilde{\xi}_\alpha$  of  $\xi_\alpha$  which satisfies (C1) and an integration procedure which satisfies (C2), (C3), we have that the numerical solution  $\tilde{\psi}$  of the initial value problem (16) satisfies*

$$\sup_{s \in \mathcal{T}} |\tilde{\psi}(s) - z_{\alpha,x}(s)| = O(\delta_n^q) + O_p(\beta_n), \quad (19)$$

where  $\delta_n = |\mathcal{T}|/n$  is the step size used in the integration procedure and  $|\mathcal{T}| = \tau$  is the length of the interval  $\mathcal{T}$ .

Theorems 1 and 2 imply that under regularity conditions, one can estimate  $z_{\alpha,x}$  using the joint kernel described in (11) setting  $\tilde{\xi} = \hat{\xi}$  and a well-behaved numerical integration procedure to obtain a uniform convergence rate of  $O(\delta_n^q) + O_p(h_n + \sqrt{\frac{\log n}{nh_n}})$ .

## 5. SIMULATION STUDY

To evaluate the performance of our method, we simulate snippet data from two simulation processes. The first is exponential in nature, generated from sample curves following  $Y(t) = \exp\{-b(t+1)\}$  where  $b$  is a  $\mathcal{U}(.3, .5)$  random variable. The second is a quadratic process, using  $Y(t) = a - bt^2$ , where  $a \sim \mathcal{U}(190, 200)$ ,  $b \sim \mathcal{U}(.2, .8)$  and  $a$  is independent of  $b$ . In both scenarios the time domain is the interval  $(0, 10)$ . Plots of a subset of underlying samples are shown in Figure 3.

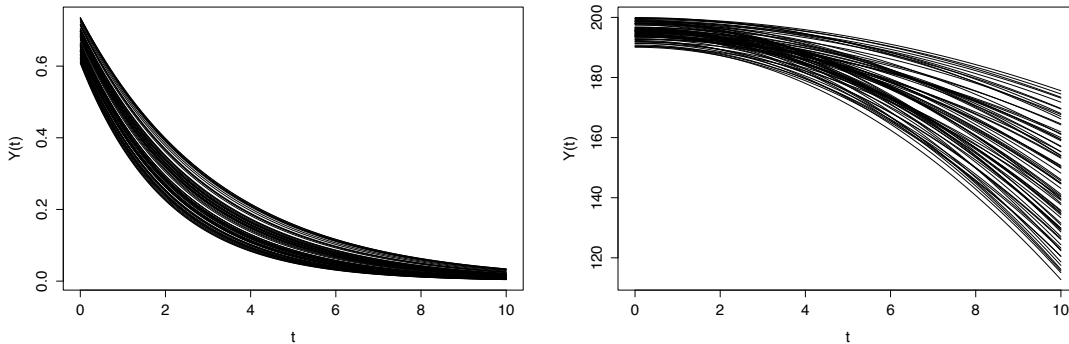


Figure 3: Subset of generated curves from the exponential (left) and quadratic (right) simulations.

The simulations are chosen to mimic natural occurring phenomena. For example, the quadratic decline process describes a situation where decline is amplified as time increases. In both simulations, we sample  $X_i = Y(T_i)$  and  $Z_i = Y'(T_i)$  with the  $T_i$  having a  $\mathcal{U}(0, 10)$  distribution. While the underlying processes are highly nonlinear, our observations only carry local linear information. However, our method allows us to pool information from all subjects to uncover the true nonlinear relationship without using any parametric assumptions.

Our simulation study examines the effect of the estimation procedure, sample size, choice of  $\alpha$ , and measurement error. The estimation procedures considered are: the binomial regression model in (7) using a logistic link, the kernel estimator in (10) with bandwidth .01 in the exponential case and 1 in the quadratic case and Gaussian kernel, and the joint kernel estimator in (11) with  $h_K = .01$  and  $h_H = .001$  in the exponential case and  $h_K = 1$  and  $h_H = .05$  in the quadratic case and Gaussian kernel. All bandwidths were chosen manually. We vary the sample size using  $n = 300$  and 1000. The probability  $\alpha$  is varied over  $\alpha = \{.05, .25, .5, .75, .95\}$ . Finally, we compare the quality of estimates with and without measurement error added to both level and derivative observations independently. To be clear, measurement error is introduced by  $(X_i + \varepsilon_{X_i}, Z_i + \varepsilon_{Z_i})$ ,

where  $\varepsilon_{X_i} \sim N(0, \sigma_X^2)$ ,  $\varepsilon_{Z_i} \sim N(0, \sigma_Z^2)$ , and  $\varepsilon_{X_i}$  is independent of  $\varepsilon_{Z_i}$ . In the exponential case we use  $\sigma_X = \sigma_Z = .01$ ; in the quadratic case we use  $\sigma_X = 2$  and  $\sigma_Z = 1$ .

As a measure of quality we consider the average integrated squared error (AISE) when repeating the simulations  $N = 100$  times. For our target  $z_{\alpha,x}(s)$  for  $s \in (0, \tau]$  and its estimator, the AISE is defined as

$$\text{AISE} = \frac{1}{100} \sum_{i=1}^{100} \int_0^{\tau} (z_{\alpha,x}(s) - \tilde{\psi}^{(i)}(s))^2 ds,$$

where  $\tilde{\psi}^{(i)}(s)$  is the functional estimate of  $z_{\alpha,x}(s)$  in the  $i^{\text{th}}$  repetition. The time domain in the exponential case is chosen to be  $(0, 8]$  since after time  $s = 8$  many of the trajectories are flat, while in the quadratic case the chosen time domain is  $(0, 5]$ . We find that the kernel type estimators outperform the logistic regression model, since the parametric model lacks flexibility. As shown in Figure 4 our methods perform quite well, even with a modest sample size of 300. As shown in the Supplement, the performance is expectedly worsened when measurement error is introduced.

Not surprisingly, Figure 4 demonstrates that the extreme quantile trajectories are more difficult to estimate, accounting for the larger spread toward the end of the time domain. The more moderate quantiles, such as the median, however, are estimated quite accurately.

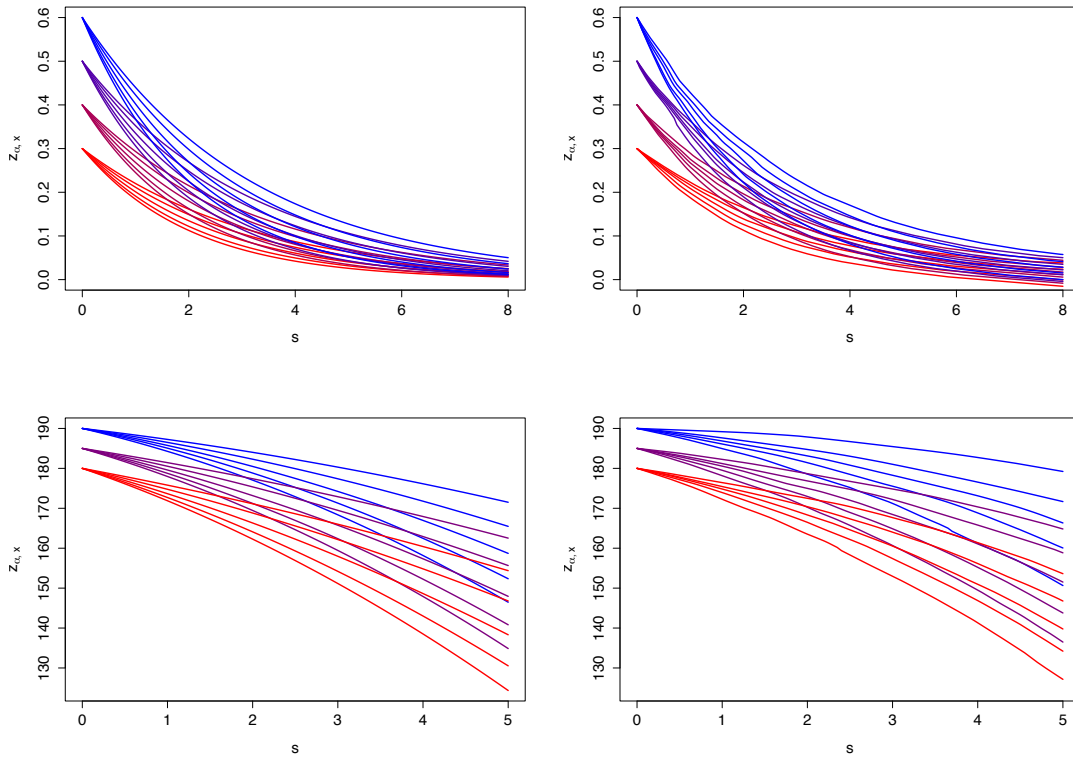


Figure 4: Results of single noiseless simulations for various starting levels, and  $\alpha \in \{.05, .25, .5, .75, .95\}$  for the exponential (top) and quadratic (bottom) cases. The left panels show the true  $z_{\alpha,x}$  while the right panels show our estimate based on a kernel estimate of  $F(z|x)$ , with a sample size of 300. For clarity, curves starting from different levels are colored differently.

A summary table of the exponential simulation study may be found in Table 1, and shows that the kernel estimators described in (10) and (11) outperform the logistic method in all cases. In the case of small sample sizes the kernel estimator shows slightly better performance over the joint kernel estimator. Median trajectories are estimated quite accurately in all scenarios in the exponential simulation, even in the presence of measurement error (see Figure 8 in the Supplement). The corresponding results for the quadratic simulation may be found in Figure 10 and Table 2 in the Supplement, where we also find that the nonparametric methods outperform the logistic model.

Noise	Sample Size	$\alpha$	Logistic Model	Kernel Smoothing	Joint Kernel
No	300	.05	6.30	.447	<b>.425</b>
		.25	.508	<b>.092</b>	.109
		.50	.184	<b>.123</b>	.161
		.75	.845	<b>.108</b>	.121
		.95	5.99	<b>.246</b>	.252
	1000	.05	6.33	<b>.456</b>	.456
		.25	.491	.054	<b>.048</b>
		.50	.155	.106	<b>.105</b>
		.75	.810	<b>.110</b>	.111
		.95	5.88	.284	<b>.280</b>
Yes	300	.05	12.5	6.71	<b>6.59</b>
		.25	.882	.570	<b>.536</b>
		.50	.191	<b>.151</b>	.201
		.75	1.64	<b>.847</b>	.942
		.95	12.1	<b>4.53</b>	4.82
	1000	.05	12.7	7.55	<b>7.22</b>
		.25	.896	.549	<b>.541</b>
		.50	.160	.118	<b>.116</b>
		.75	1.59	.811	<b>.796</b>
		.95	12.1	4.86	<b>4.78</b>

Table 1: AISE scores ( $\times 1000$ ) for various scenarios in the exponential simulation, each with a starting value of  $x = 0.4$ .

## 6. APPLICATION TO ALZHEIMER'S DATA

We now return to the motivating dataset consisting of hippocampal volume measurements. The dataset of interest contains measurements of longitudinal hippocampal volumes for 270 subjects, with ages ranging from 47 to 96. We remove subjects whose trajectories are increasing (8 demented, 18 MCI, and 29 normal subjects removed). Demented and MCI subjects are pooled, forming a cognitively impaired group. For these data we estimate the  $z_{\alpha,x}$  for varying levels of  $\alpha$  and starting points  $x$ . As the kernel estimator performed best in the simulation study, we use it as our estimation method. Our results align with intuition and previous scientific findings. For example, Figure 5 shows that the decline rate is more severe for the demented and MCI groups than it is for the normal group.

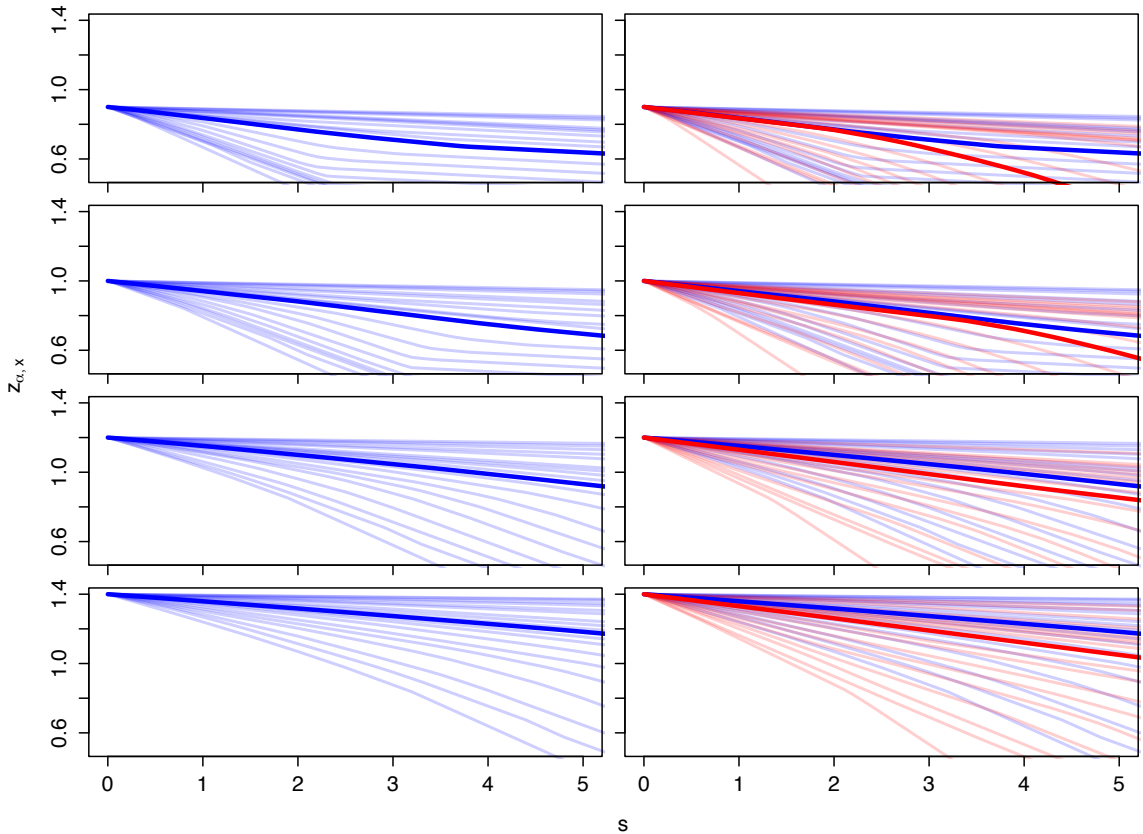


Figure 5: Estimated quantile trajectories for normal and MCI/demented groups, where  $\alpha \in \{.05, \dots, .95\}$ , using the kernel method with bandwidth .12, chosen manually, and Gaussian kernel. From top to bottom the starting points are varied; from left to right the impaired group is overlaid onto the normal group for clarity in comparison. Median trajectories are shown in bold.

Another interesting result is that the atrophy is accelerating for lower levels, especially among the demented subjects. This characteristic implies that affected subjects are getting worse, which is a confirmation of what has already been documented in Alzheimer's studies. For instance see Sabuncu et al. (2011) in which the authors caution practitioners from ignoring the nonlinear trend in hippocampal atrophy. Figure 5 shows clear differences in distribution for the two groups. The highest quantile trajectories for the normal groups are uniformly higher than the corresponding trajectories in the cognitively im-

paired group. A similar pattern is seen in the lowest quantile trajectories. From this model we are able to estimate future potential trajectories in a data driven way and gain access to underlying smooth nonlinear features in the data.

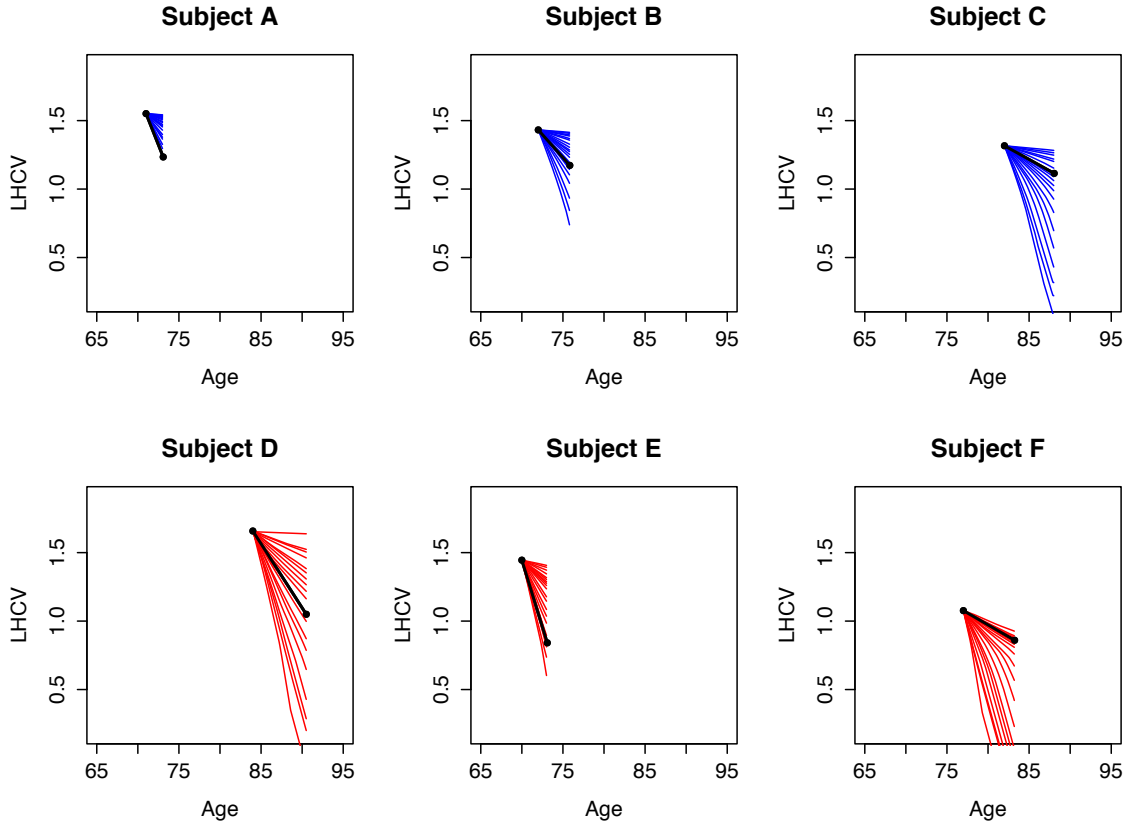


Figure 6: A subset of six individual snippets with corresponding  $z_{\alpha,x}$  trajectories originating from the first observation point for each subject. Here,  $\alpha \in \{.05, \dots, .95\}$ . The black dots are actual observations for each subject; each of these subjects has two observations. The subjects in the top row are from the normal group while the subjects on the bottom row are from the cognitively impaired group.

The plots in Figure 5 represent estimates of population conditional quantiles. We can use this information to examine the severity of a given subject’s trajectory. For this we estimate  $z_{\alpha,x}$  starting from the subject’s first observation. A demonstration of this procedure on a representative sample of six individuals (3 in each cognitive group)

is shown in Figure 6. This approach offers a useful way to evaluate an individual’s trajectory, based on pooling information from the entire sample. For example, one can see that Subject A is on a very severe trajectory with respect to the normal cognitive group. On the other hand Subject F, though cognitively impaired, is only on a mild decline relative to the cognitively impaired.

We can take our analysis a step further in making predictions about a subject’s future trajectories. The idea is to estimate  $z_{\alpha,x}$  trajectories for various  $\alpha$  starting from the subject’s last measurement. To ensure that the trajectories align with the subject’s snippet, we require that the quantile trajectories do not deviate too much near the last observation. To achieve this, we first calculate the quantile on which the subject is traveling, and then employ quantile trajectories where  $\alpha = \alpha(s)$  depends on the time difference between the prediction and the subject’s last observation.

Specifically, if a subject’s snippet is traveling at a given quantile  $\alpha^*$ , in estimating the  $\alpha$  quantile trajectory we define

$$\alpha(s) = \begin{cases} (\alpha - \alpha^*)/s & \text{if } s < S^* \\ \alpha & \text{if } s \geq S^* \end{cases}, \quad (20)$$

where  $S^*$  controls how long the prediction trajectory must adhere to the subject’s snippet. In practice, we choose a subject specific  $S_i^* = \frac{1}{2}(A_{in_i} - A_{i1})$  to reflect the length of the subject’s snippet. We estimate  $\alpha^*$  by comparing a subject’s slope  $Z_i$  to the estimated conditional distribution  $\tilde{F}_K(z|y_{i,n_i})$ , where  $y_{i,n_i}$  is the subject’s last observation. An illustration of  $\alpha(s)$  can be found in Figure 11 in the Supplement.

In Figure 7, we demonstrate a useful application of these predicted quantile trajectories. For each subject, we estimate the trajectory if a subject were to remain at the same quantile  $\alpha^*$  throughout; this curve is shown in black. Additionally, we estimate a range

of  $\alpha$  quantile trajectories under the constraint that early in the prediction, each  $\alpha$  must be close to  $\alpha^*$ . After time  $S_i^*$ , the  $\alpha$  quantile trajectories are unconstrained.

To demonstrate our prediction method, we use the same six individuals as in Figure 6. Prediction in this way is flexible and allows one to pool information from the sample while simultaneously enforcing a degree of compliance with a subject's snippet measurements.

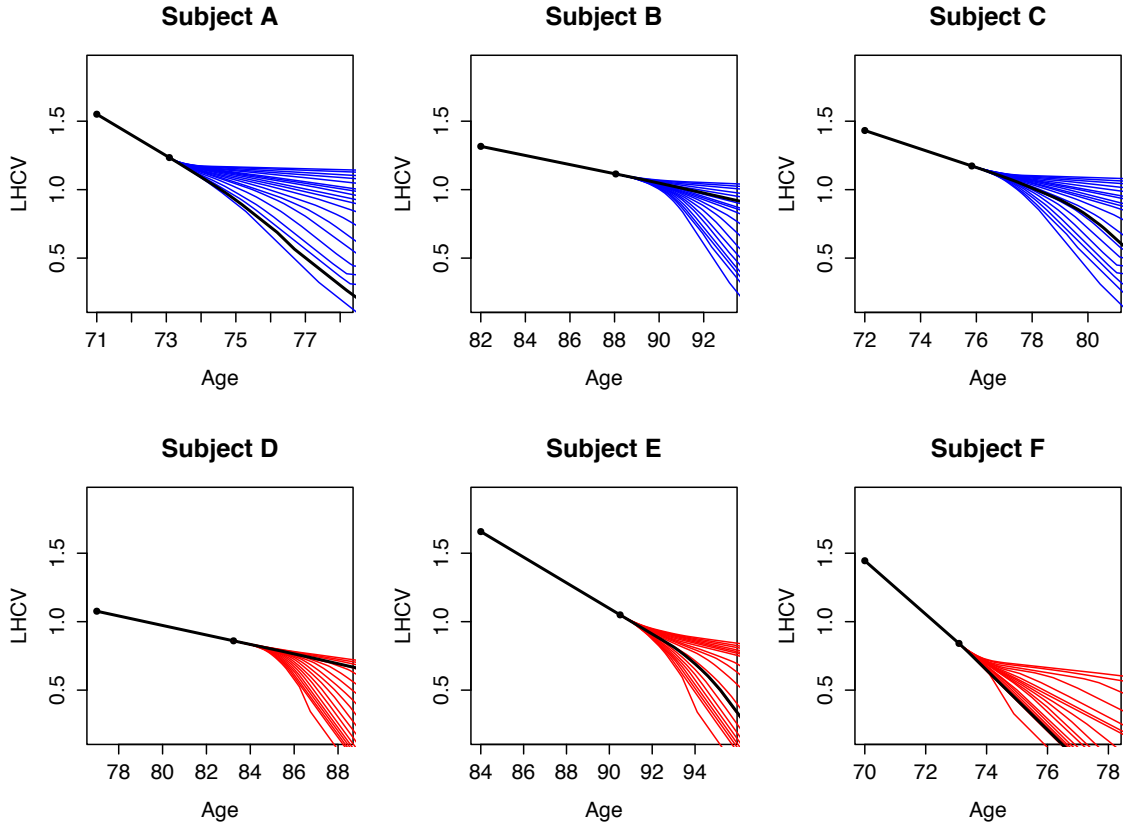


Figure 7:  $\alpha$ -quantile prediction trajectories where  $S^*$  is chosen to be half the length of timespan of the subject's snippet. The black curves that continue the original observed data snippet which correspond to the linear initial part represent estimated  $\alpha^*$  prediction trajectories, where  $\alpha^*$  is the estimated quantile of slopes for each subject, conditioned on their last observation. The black dots are the subjects' actual measurements.

## 7. DISCUSSION

The problem of longitudinal snippet data is common, especially in medical or social science

studies where dense measurements over a long period of time are often not available due to logistical problems. In our analysis of snippet data we also face a lack of information about absolute time, which is also common in snippet data. This makes it more difficult to assess the dynamics of the underlying process and we demonstrate here how one can use the available relative time markers to identify a dynamical system that generates the data. Our approach relies on monotonicity of the underlying processes, which makes it possible to adopt the level of the process as a reference as opposed to time, which circumvents the lack of information about absolute time. This novel approach motivates to consider conditional quantile trajectories and their estimation, given an initial value. We demonstrate that the implementation of this idea is straightforward and provide theoretical support.

While our methods have been motivated by the challenges posed by an Alzheimer's dataset, we note that taking this alternative view may have benefits for many other analyses of functional or longitudinal data. Instead of examining curves over time, in the monotonic case one can model curves over level. This is reasonable when the process depends more on its current level than it does on its current time, as likely is the case with Alzheimer's disease, where anyway the relevant disease duration that corresponds to absolute time (rather than age of a subject) is simply not available in many studies.

The proposed methods may also prove useful in and can be easily adapted to the case where (absolute) time is actually available. For example, in the logistic models described in (7) and (8) as well as in the nonparametric settings of (10) and (11), age or any other time variable can be easily included in the model as an additional covariate. Our methods and especially the instantaneous  $\alpha$ -quantile and the resulting  $\alpha$ -quantile trajectory provide useful information about the dynamics of very sparsely observed processes. The proposed estimates perform well and this method will be a useful tool to recover and predict conditional time-dynamic processes in the presence of limited data.

## REFERENCES

- Abramson, I. and Müller, H.-G. (1994), “Estimating direction fields in autonomous equation models, with an application to system identification from cross-sectional data,” *Biometrika*, 81, 663–672.
- Albert, M. S., DeKosky S. T., Dickson D., Dubois, B., Feldman, H. H. Feldman, Fox, N. C., Gamst, A., Holtzman, D. M., Jagust, W. J., Petersen, R. C., Snyder, P. J., Carillo, M. C., Thies, B., Phelps, C. H (2011), “The diagnosis of mild cognitive impairment due to Alzheimer’s disease: recommendations from the National Institute on Aging-Alzheimer’s Association workgroups on diagnostic guidelines for Alzheimer’s disease,” *Alzheimer’s & Dementia : The Journal of the Alzheimer’s Association*, 7, 270–279.
- Delaigle, A. and Hall P. (2013), “Classification using censored functional data,” *Journal of the American Statistical Association*, 108, 1269–1283.
- Fan, J. and Gijbels, I. (1996), *Local polynomial modelling and its applications*, Chapman & Hall/CRC.
- Ferraty, F., Laksaci, A., Vieu, P. (2006), “Estimating some characteristics of the conditional distribution in nonparametric functional models,” *Statistical Inference for Stochastic Processes*, 9, 47–76.
- Gragg, W.B.(1965), “On extrapolation algorithms for ordinary initial value problems,” *Journal of the Society for Industrial and Applied Mathematics: Series B, Numerical Analysis*, 2, 384–403.
- Hall, P., Wolff, R. C., Yao, Q. (1999), “Methods for estimating a conditional distribution function,” *Journal of the American Statistical Association*, 94, 154–163.
- Hansen, B. E. (2008) “Uniform convergence rates for kernel estimation with dependent data,” *Econometric Theory*, 24, 726–748.

- Härdle, W., Janssen, P., Serfling, R. (1988), “Strong uniform consistency rates for estimators of conditional functionals,” *The Annals of Statistics*, 16, 1428–1499.
- Horrigue, W. and Saïd, E. O. (2011), “Strong uniform consistency of a nonparametric estimator of a conditional quantile for censored dependent data and functional regressors,” *Random Operators and Stochastic Equations*, 19, 131–156.
- Kraus, D. (2015), “Components and completion of partially observed functional data,” *Journal of the Royal Statistical Society: Series B (Statistical Methodology)*, 77, 777–801.
- Li, Q. and Racine, J. S. (2008), “Nonparametric estimation of conditional CDF and quantile function with mixed categorical and continuous data,” *Journal of Business and Economic Statistics*, 26, 423–434.
- McKhann, G. M., Knopman, D. S., Chertkow, H., Hyman, B. T., Clifford, J., Jack, C.R. Jr., Kawas, C. H., Klunk, W. E., Koroshetz, W. J., Manly, J. J., Mayeux, R., Mohs, R. C., Morris, J. C., Rossor, M. N., Scheltens, P., Carrillo, M. C., Thies, B., Weintraub, S., Phelps, C. H. (2011), “The diagnosis of dementia due to Alzheimer’s disease: recommendations from the National Institute on Aging-Alzheimer’s Association workgroups on diagnostic guidelines for Alzheimer’s disease,” *Alzheimer’s & Dementia : the Journal of the Alzheimer’s Association*, 7, 263–269.
- Mu, Y. and Gage, F. (2011) “Adult hippocampal neurogenesis and its role in Alzheimer’s disease,” *Molecular Neurodegeneration*, 6:85.
- Mungas, D., Reed, B., Crane, P., Haan, M., González H. (2004), “Spanish and English Neuropsychological Assessment Scales (SENAS): further development and psychometric characteristics,” *Psychological Assessment*, 16, 347–359.
- Ramsay, J. O. and Silverman, B. W. (2005), *Functional Data Analysis*, Springer Series in Statistics, New York: Springer, 2nd ed.
- Roussas, G. (1969), “Nonparametric estimation of the transition distribution function of a Markov process” *The Annals of Mathematical Statistics*, 40, 1386–1400.

- Sabuncu, M.R., Desikan, R.S., Sepulcre, J., Yeo, B.T., Liu, H., Schmansky, N.J., Reuter, M., Weiner, M.W., Buckner, R.L., Sperling, R.A., Fischl, B. (2011), “The dynamics of cortical and hippocampal atrophy in Alzheimer’s disease,” *Archives of Neurology*, 68, 1040–1048.
- Samanta, M. (1989), “Non-parametric estimation of conditional quantiles,” *Statistics and Probability Letters*, 7, 407–412.
- Sperling, R. A., Aisen, P. S., Beckett, L. A., Bennett, D. A., Craft, S., Fagan, A. M., Iwatsubo, T., Jack, C. R. Jr., Montine, T. J., Park, D. C., Reiman, E. M., Rowe, C. C., Siemers, E., Stern, Y., Yaffe, K., Carrillo, M. C., Thies, B., Morrison-Bogorad, M., Wagster, M. V., Phelps, C. H. Phelps (2011), “Toward defining the preclinical stages of Alzheimer’s disease: recommendations from the National Institute on Aging-Alzheimer’s Association workgroups on diagnostic guidelines for Alzheimer’s disease,” *Alzheimer’s & Dementia : The Journal of the Alzheimer’s Association*, 7, 280–292, 2011.
- Yao, F., Müller, H.-G., and Wang, J.-L. (2005), “Functional data analysis for sparse longitudinal data,” *Journal of the American Statistical Association*, 100, 577–590.

SUPPLEMENT: PROOFS

**Proof of Proposition 1:** At  $t = 0$  the conditional quantile must be equal to  $x$ , i.e.,

$$q_{\alpha,x}(T + 0) = x.$$

This must be the case since the conditional quantile is based on a starting value of  $Y(T) = x$ . Next, since  $q_{\alpha,x}$  is smooth, it must hold that

$$\frac{dq_{\alpha,x}(T + 0)}{dt} = \xi_{\alpha}(x),$$

i.e., the slope of the cross-sectional quantile trajectory at  $t = 0$  must equal the  $\alpha$ -quantile of slopes at  $t = 0$ . From these two facts we have that the slope field that describes the behavior of  $q_{\alpha,x}$  at  $t = 0$  is made up of conditional  $\alpha$ -quantiles of slopes, since we can condition on any level  $x \in \mathcal{J}$ . Now since the differential equation is autonomous, the starting time is arbitrary so for all  $t \in \mathcal{T}$ , and for all possible starting levels  $x$ , we have that the conditional cross-sectional quantile must travel on the conditional  $\alpha$ -quantile of slopes. This behavior precisely defines the  $\alpha$ -ICQ  $z_{\alpha,x}$ .

**Proof of Theorem 1:** Equation (18) is a direct consequence of theorems in Ferraty et al. (2006) and Horrigue and Saïd (2011).

For (18), by the Implicit Function Theorem, we have

$$\xi_{\alpha}'(x) = -\frac{\partial F(z|x)}{\partial x} \times \left( \frac{\partial F(z|x)}{\partial z} \right)^{-1} \Big|_{z=\xi_{\alpha}(x)}$$

and

$$\tilde{\xi}_{\alpha}'(x) = -\frac{\partial \tilde{F}_{SNW}(z|x)}{\partial x} \times \left( \frac{\partial \tilde{F}_{SNW}(z|x)}{\partial z} \right)^{-1} \Big|_{z=\tilde{\xi}_{\alpha}(x)}.$$

Using the convention that  $F^{(i,j)}(x, z) = \frac{\partial F(x, z)}{\partial x^i \partial z^j}$  where  $F(x, z)$  is the two-dimensional

c.d.f. of  $(X, Z)$ , this leads to

$$\begin{aligned}\xi'_\alpha(x) &= \frac{f'_X(x)F^{(1,0)}(x, z) - f_X(x)F^{(2,0)}(x, z)}{[f_X(x)]^2} \times \frac{f_X(x)}{F^{(1,1)}(x, z)} \Big|_{z=\xi_\alpha(x)} \\ &= \frac{F^{(1,0)}(x, z)f'_X(x) - F^{(2,0)}(x, z)f_X(x)}{f_{X,Z}(x, z)f_X(x)} \Big|_{z=\xi_\alpha(x)}\end{aligned}\quad (21)$$

where  $f_X(x)$  is the marginal p.d.f. of  $X$  and  $f_{X,Z}(x, z)$  is the joint p.d.f. of  $(X, Z)$ .

Applying the same method to the estimator, we have

$$\begin{aligned}\tilde{\xi}'_\alpha(x) &= \frac{\sum_{i=1}^n H\left(\frac{z-Z_i}{h}\right)K\left(\frac{x-X_i}{h}\right) \sum_{i=1}^n K'\left(\frac{x-X_i}{h}\right) - \sum_{i=1}^n H\left(\frac{z-Z_i}{h}\right)K'\left(\frac{x-X_i}{h}\right) \sum_{i=1}^n K\left(\frac{x-X_i}{h}\right)}{\sum_{i=1}^n K\left(\frac{z-Z_i}{h}\right)K\left(\frac{x-X_i}{h}\right) \sum_{i=1}^n K\left(\frac{x-X_i}{h}\right)} \Big|_{z=\tilde{\xi}_\alpha(x)} \\ &= \frac{\tilde{F}^{(1,0)}(x, z)\tilde{f}'_X(x) - \tilde{F}^{(2,0)}(x, z)\tilde{f}_X(x)}{\tilde{f}_{X,Z}(x, z)\tilde{f}_X(x)} \Big|_{z=\tilde{\xi}_\alpha(x)},\end{aligned}\quad (22)$$

where

$$\begin{aligned}\tilde{F}^{(1,0)}(x, z) &:= \frac{1}{nh} \sum_{i=1}^n H\left(\frac{z-Z_i}{h}\right)K\left(\frac{x-X_i}{h}\right) \\ \tilde{f}_{X,Z}(x, z) &:= \frac{1}{nh^2} \sum_{i=1}^n K\left(\frac{x-X_i}{h}\right)K\left(\frac{z-Z_i}{h}\right) \\ \tilde{f}'_X(x) &:= \frac{1}{nh^2} \sum_{i=1}^n K'\left(\frac{x-X_i}{h}\right) \\ \tilde{f}_X(x) &:= \frac{1}{nh} \sum_{i=1}^n K\left(\frac{x-X_i}{h}\right)\end{aligned}$$

*Lemma:* Under the conditions of Theorem 1, we have

1.  $\sup_{x \in \mathcal{J}} |f_X(x) - \tilde{f}_X(x)| = o_p(1)$
2.  $\sup_{x \in \mathcal{J}} |f'_X(x) - \tilde{f}'_X(x)| = o_p(1)$
3.  $\sup_{x \in \mathcal{J}} \sup_{z \in \mathcal{Z}} |f_{X,Z}(x, z) - \tilde{f}_{X,Z}(x, z)| = o_p(1)$
4.  $\sup_{x \in \mathcal{J}} \sup_{z \in \mathcal{Z}} |F^{(1,0)}(x, z) - \tilde{F}^{(1,0)}(x, z)| = o_p(1)$
5.  $\sup_{x \in \mathcal{J}} \sup_{z \in \mathcal{Z}} |F^{(2,0)}(x, z) - \tilde{F}^{(2,0)}(x, z)| = o_p(1)$

*Proof of Lemma:* Items (i) - (iii) follow immediately from Hansen (2008), while (iv) follows from Samanta (1989). Proving (v) involves only a slight modification of the proof to (iv).

Next, define the numerator in (21) as

$$p(x, z) := F^{(1,0)}(x, z)f'_X(x) - F^{(2,0)}(x, z)f_X(x)$$

and similarly from 22 define

$$\tilde{p}(x, z) := \tilde{F}^{(1,0)}(x, z)\tilde{f}'_X(x) - \tilde{F}^{(2,0)}(x, z)\tilde{f}_X(x).$$

Also define these denominators as

$$q(x, z) := f_{X,Z}(x, z)f_X(x)$$

$$\tilde{q}(x, z) := \tilde{f}_{X,Z}(x, z)\tilde{f}_X(x).$$

The lemma implies that

$$\sup_{x \in \mathcal{J}} \sup_{z \in \mathcal{Z}} |p(x, z) - \tilde{p}(x, z)| = o_p(1)$$

$$\sup_{x \in \mathcal{J}} \sup_{z \in \mathcal{Z}} |q(x, z) - \tilde{q}(x, z)| = o_p(1).$$

Next write

$$\tilde{\xi}'_\alpha(x) = \frac{\tilde{p}(x, \tilde{\xi}_\alpha(x))/q(x, \tilde{\xi}_\alpha(x))}{\tilde{q}(x, \tilde{\xi}_\alpha(x))/q(x, \tilde{\xi}_\alpha(x))},$$

and note that the lemma implies that

$$\begin{aligned} \sup_{x \in \mathcal{J}} \sup_{z \in \mathcal{Z}} \left| \frac{\tilde{q}(x, z)}{q(x, z)} - 1 \right| &= \sup_{x \in \mathcal{J}} \sup_{z \in \mathcal{Z}} \left| \frac{\tilde{q}(x, z) - q(x, z)}{q(x, z)} \right| \\ &\leq \frac{\sup_{x \in \mathcal{J}} \sup_{z \in \mathcal{Z}} |\tilde{q}(x, z) - q(x, z)|}{\delta_1 \delta_2} = o_p(1). \end{aligned}$$

Now

$$\sup_{x \in \mathcal{J}} \sup_{z \in \mathcal{Z}} \left| \frac{\tilde{p}(x, z)}{q(x, z)} - \frac{p(x, z)}{q(x, z)} \right| = \sup_{x \in \mathcal{J}} \sup_{z \in \mathcal{Z}} \left| \frac{\tilde{p}(x, z) - p(x, z)}{q(x, z)} \right| = o_p(1).$$

Since  $\frac{\tilde{p}(x, z)}{q(x, z)}|_{z=\tilde{\xi}_\alpha(x)} = \tilde{\xi}'_\alpha(x)$  and  $\frac{p(x, z)}{q(x, z)}|_{z=\xi_\alpha(x)} = \xi'_\alpha(x)$ , we have that

$$\tilde{\xi}'_\alpha(x) = \xi'_\alpha(x) + o_p(1),$$

uniformly in  $x$ .

**Proof of Theorem 2:** First we discuss the existence of unique solutions to the equations

$$\frac{dz_{\alpha, x}(s)}{ds} = \xi_\alpha(z_{\alpha, x}(s)), \quad z_{\alpha, x}(0) = x \quad (23)$$

and

$$\frac{d\tilde{z}_{\alpha, x}(s)}{ds} = \tilde{\xi}_\alpha(\tilde{z}_{\alpha, x}(s)), \quad \tilde{z}_{\alpha, x}(0) = x. \quad (24)$$

for  $s \in \mathcal{T} = [0, T_1]$  for some  $0 < T_1 < \infty$ . By the assumptions of the theorem, we have that the functions  $\xi_\alpha$  and  $\tilde{\xi}_\alpha$  are continuously differentiable over  $\mathcal{J}$ . It is well known that under these conditions that unique solutions exist to both (23) and (24).

As we are interested in the quantity  $\sup_{s \in \mathcal{T}} |\tilde{\psi}(s) - z_{\alpha, x}(s)|$ , that is, the supremum difference between the target and its estimate using  $\tilde{\xi}_\alpha$  and some integration procedure, we have

$$\begin{aligned} \sup_{s \in \mathcal{T}} |\tilde{\psi}(s) - z_{\alpha, x}(s)| &\leq \sup_{s \in \mathcal{T}} |\tilde{\psi}(s) - \tilde{z}_{\alpha, x}(s)| + \sup_{s \in \mathcal{T}} |\tilde{z}_{\alpha, x}(s) - z_{\alpha, x}(s)| \\ &= S_1 + S_2 \end{aligned} \quad (25)$$

The quantity  $S_1$  can be taken care of by the fact that  $\tilde{\psi}$  is the numerical approximation of  $\tilde{z}_{\alpha, x}$ . Since the integration procedure is assumed to be of order  $q$ , it follows that  $S_1 = O(\delta_n^q)$  (see the proof of the theorem in Abramson and Müller (1994)).

As for  $S_2$ , consider a sequence of  $m$  starting points  $s_i = \frac{(i-1)T_1}{m}$  for  $i = 1, \dots, m$  and the following initial value problems with different starting levels:

$$\begin{aligned} \frac{dz_{\alpha,x}(s)}{ds} &= \xi_{\alpha}(z_{\alpha,x}(s)), & z_{\alpha,x}(s_i) &= z_{i1}, & s &\geq s_i \\ \frac{dz_{\alpha,x}(s)}{ds} &= \xi_{\alpha}(z_{\alpha,x}(s)), & z_{\alpha,x}(s_i) &= z_{i2}, & s &\geq s_i \end{aligned} \quad (26)$$

Denote the solutions to these equations as  $z_{\alpha,x}(s; z_{i1})$  and  $z_{\alpha,x}(s; z_{i2})$ , respectively. These solutions depend continuously on the initial conditions  $z_{i1}$  and  $z_{i2}$  and so there exists a constant  $C_1 > 0$  such that

$$|z_{\alpha,x}(s_{i+1}; z_{i1}) - z_{\alpha,x}(s_{i+1}; z_{i2})| \leq C_1 |z_{i1} - z_{i2}| \quad (27)$$

for  $i = 1, \dots, m$ . This controls the difference between two solutions with different initial conditions. Next consider a third initial value problem

$$\frac{d\tilde{z}_{\alpha,x}(s)}{ds} = \tilde{\xi}_{\alpha}(\tilde{z}_{\alpha,x}(s)), \quad \tilde{z}_{\alpha,x}(s_i) = \tilde{z}_i \quad s \geq s_i, \quad (28)$$

and denote the solution to this equation as  $\tilde{z}_{\alpha,x}(s; \tilde{z}_i)$ . Next we bound the quantity

$$\sup_{s_i \leq s \leq s_{i+1}} |z_{\alpha,x}(s; \tilde{z}_i) - \tilde{z}_{\alpha,x}(s; \tilde{z}_i)|.$$

By making use of a Taylor expansion, and noting that at the starting time  $s_i$ , the two functions  $z_{\alpha,x}$  and  $\tilde{z}_{\alpha,x}$  are the same at  $\tilde{z}_i$ , we have that

$$\begin{aligned} z_{\alpha,x}(s; \tilde{z}_i) - \tilde{z}_{\alpha,x}(s; \tilde{z}_i) &= z_{\alpha,x}(s_i; \tilde{z}_i) - \tilde{z}_{\alpha,x}(s_i; \tilde{z}_i) \\ &\quad + (s - s_i)(z'_{\alpha,x}(s_i; \tilde{z}_i) - \tilde{z}'_{\alpha,x}(s_i; \tilde{z}_i)) \\ &\quad + \frac{(s - s_i)^2}{2}(z''_{\alpha,x}(\zeta; \tilde{z}_i) - \tilde{z}''_{\alpha,x}(\zeta; \tilde{z}_i)), \end{aligned}$$

for some  $\zeta \in (s_i, s)$ , which leads to

$$\sup_{s_i \leq s \leq s_{i+1}} |z_{\alpha,x}(s; \tilde{z}_i) - \tilde{z}_{\alpha,x}(s; \tilde{z}_i)| \leq \frac{C_2}{m} |\xi_\alpha(\tilde{z}_i) - \tilde{\xi}_\alpha(\tilde{z}_i)| + \frac{C_3}{m^2} (C_4 + \sup_{x \in \mathcal{J}} |\xi'_\alpha(x) - \tilde{\xi}'_\alpha(x)|), \quad (29)$$

for  $0 \leq i \leq m$  and constants  $C_2, C_3, C_4 > 0$ .

Now we have a way of controlling the difference between two different solutions given the same initial condition. We can put this together with (27) to get an overall upper bound. First notice that for  $s \geq s_i$ , we have

$$\begin{aligned} \tilde{z}_{\alpha,x}(s) &= \tilde{z}_{\alpha,x}(s; \tilde{z}_{\alpha,x}(s_i)) \\ z_{\alpha,x}(s) &= z_{\alpha,x}(s; z_{\alpha,x}(s_i)). \end{aligned} \quad (30)$$

Then for  $0 \leq i \leq m$ , we have

$$\begin{aligned} \sup_{s_i \leq s \leq s_{i+1}} |z_{\alpha,x}(s) - \tilde{z}_{\alpha,x}(s)| &\leq \sup_{s_i \leq s \leq s_{i+1}} |\tilde{z}_{\alpha,x}(s; \tilde{z}_{\alpha,x}(s_i)) - z_{\alpha,x}(s; \tilde{z}_{\alpha,x}(s_i))| \\ &\quad + \sup_{s_i \leq s \leq s_{i+1}} |z_{\alpha,x}(s; z_{\alpha,x}(s_i)) - z_{\alpha,x}(s; \tilde{z}_{\alpha,x}(s_i))| \\ &\leq O_p\left(\frac{\beta_n}{m}\right) + O_p\left(\frac{C_3 C_4 + 1}{m^2}\right) + C_1 |z_{\alpha,x}(s_i) - \tilde{z}_{\alpha,x}(s_i)|, \end{aligned} \quad (31)$$

where the  $O_p$  terms are uniform in  $i$ . If we choose  $m = n$ , then it follows that

$$|\tilde{z}_{\alpha,x}(s_{i+1}) - z_{\alpha,x}(s_{i+1})| \leq O_p\left(\frac{\beta_n}{n}\right) + C_1 |z_{\alpha,x}(s_i) - \tilde{z}_{\alpha,x}(s_i)|.$$

Since the two functions  $z_{\alpha,x}$  and  $\tilde{z}_{\alpha,x}$  have the same initial condition of  $x$  at time  $s_0 = 0$ , we have

$$\sup_{1 \leq i \leq n} |\tilde{z}_{\alpha,x}(s_i) - z_{\alpha,x}(s_i)| = O_p(\beta_n),$$

and therefore

$$\sup_{s_i \leq s \leq s_{i+1}} |\tilde{z}_{\alpha,x}(s) - z_{\alpha,x}(s)| = O_p(\beta_n),$$

which, since this result is uniform in  $i$ , implies

$$\sup_{s \in \mathcal{T}} |\tilde{z}_{\alpha,x}(s) - z_{\alpha,x}(s)| = O_p(\beta_n).$$

### SUPPLEMENT: ADDITIONAL MATERIALS

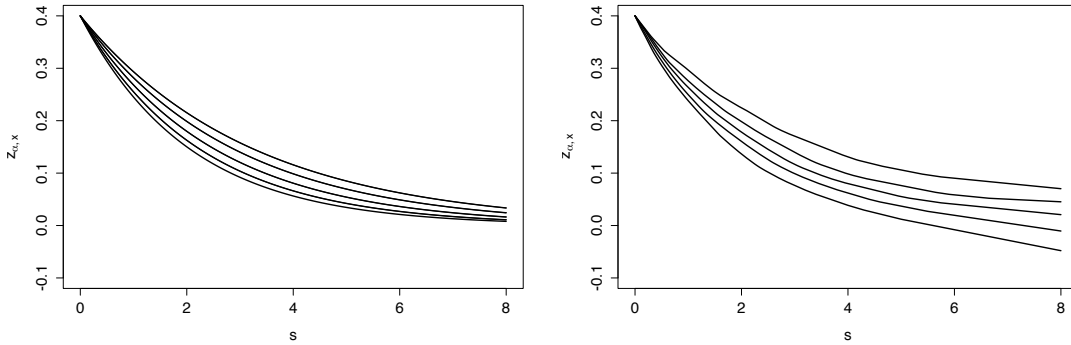


Figure 8: Simulation results in scenario (a) starting from  $x = 0.4$  using the kernel method with bandwidth  $h = .01$  and Gaussian kernel, noise added and a sample size of 300 for  $\alpha \in \{.05, .25, .50, .75, .95\}$ , showing that even in the presence of some measurement error the estimation is reasonable.

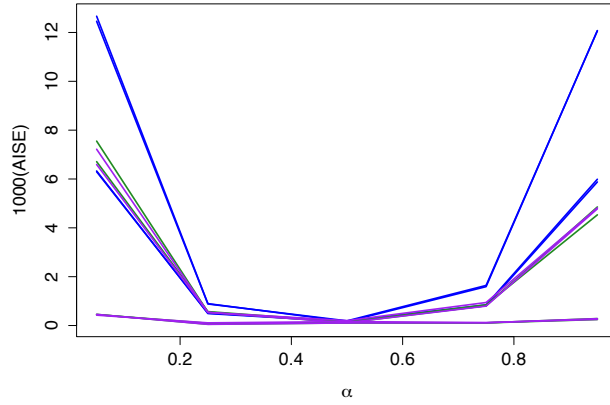


Figure 9: Comparison of AISE in the exponential simulation for different estimation methods for varying levels of  $\alpha$ , where the green are the kernel fits, purple are joint kernel fits, and the blue are logistic model fits. In general the kernel type estimators outperform the logistic model, while all methods successfully estimate the median trajectory.

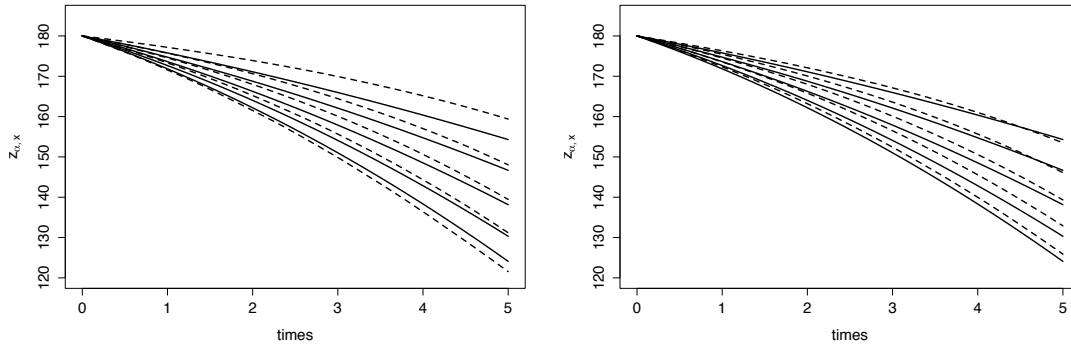


Figure 10: Averages of 100 repetitions of the quadratic simulation using a kernel estimate for  $F(z|x)$  and a sample size of 300, comparing performance with (left) and without (right) adding measurement error. Solid curves are true  $\alpha$ -quantile trajectories for  $\alpha \in \{.05, .25, .50, .75, .95\}$ ; their estimates are shown with dashed lines.

Noise	Sample Size	$\alpha$	Logistic Model	Kernel Smoothing	Joint Kernel
No	300	.05	1.66	<b>.927</b>	1.74
		.25	6.06	<b>2.25</b>	2.30
		.50	3.18	<b>1.65</b>	1.66
		.75	.845	<b>.751</b>	.830
		.95	2.37	<b>.476</b>	.501
	1000	.05	1.56	<b>.644</b>	.671
		.25	6.11	1.62	<b>1.61</b>
		.50	3.24	<b>1.18</b>	1.23
		.75	.862	<b>.632</b>	.658
		.95	2.48	<b>.541</b>	.542
Yes	300	.05	1.17	1.37	<b>.459</b>
		.25	3.26	<b>1.03</b>	1.25
		.50	3.47	<b>1.81</b>	1.93
		.75	2.76	<b>2.03</b>	2.19
		.95	13.3	<b>6.99</b>	9.19
	1000	.05	<b>1.03</b>	1.21	1.17
		.25	3.21	<b>.715</b>	.745
		.50	3.46	<b>1.43</b>	1.56
		.75	2.75	<b>1.70</b>	1.93
		.95	13.4	<b>7.72</b>	8.28

Table 2: AISE scores ( $\times 0.1$ ) for various scenarios in the quadratic simulation study, each with a starting value of  $x = 180$ .

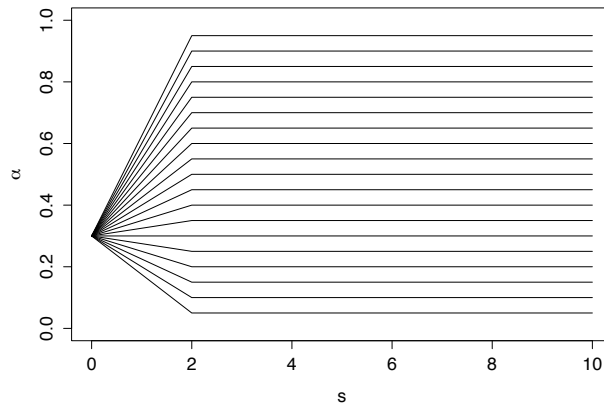


Figure 11: A demonstration of  $\alpha(s)$  for  $\alpha \in \{.05, \dots, .95\}$ , starting from  $\alpha^* = 0.3$  and with  $S^* = 2$ .